

Supplementary Material for

**An innovative S-scheme  $\text{PhC}_2\text{Cu}/\text{Ag}/\text{Ag}_2\text{MoO}_4$  photocatalyst for efficient degradation of sulfamethazine antibiotics: Heterojunctions and innergenerated  $\text{H}_2\text{O}_2$  promote radical production**

*Danluo Liang*<sup>a</sup>, *Zili Lin*<sup>a</sup>, *Yuliang Wu*<sup>b</sup>, *Daguang Li*<sup>a</sup>, *Jiayi Chen*<sup>a</sup>, *Xiaoyu Jin*<sup>a</sup>,  
*Yingyi Chen*<sup>a</sup>, *Jinfan Zhang*<sup>a</sup>, *Haijin Liu*<sup>c</sup>, *Ping Chen*<sup>a</sup>, *Wenying Lv*<sup>a</sup>, *Guoguang Liu*  
<sup>a\*</sup>.

<sup>a</sup> Guangdong Key Laboratory of Environmental Catalysis and Health Risk Control, Guangdong-HongKong-Macao Joint Laboratory for Contaminants Exposure and Health, School of Environmental Science and Engineering, Guangdong University of Technology, Guangzhou, 510006, China

<sup>b</sup> School of Civil and Environmental Engineering, Harbin Institute of Technology, Shenzhen, 518000, China

<sup>c</sup> School of Environment, Henan Normal University, Key Laboratory for Yellow River and Huaihe River Water Environment and Pollution Control, Xinxiang 453007, China

**\* Corresponding Author:** Guoguang Liu

E-mail: [liugg615@163.com](mailto:liugg615@163.com)

Tel: +86-20-39322547

Fax: +86-20-39322548

Totally 31 pages containing 7 texts, 3 tables, and 11 figures.

## TABLE OF CONTENTS

### TEXTS

Text S1. Chemical reagents.....	4
Text S2. Characterization methods .....	5
Text S3. Photocatalytic test and determination of SMT concentration .....	7
Text S4. Active species quantified and contributions rates of the ROS .....	8
Text S5. Detection of H <sub>2</sub> O <sub>2</sub> .....	9
Text S6. The methods of theoretical calculations .....	10
Text S7. Identification of photocatalytic degradation intermediates .....	11

### TABLES

Table S1. The fitted fluorescence decay components of PhC <sub>2</sub> Cu and PAM40. ....	13
Table S2. Comparison of reported literature on photocatalytic reduction of SMT .....	14
Table S3. Transformation products from the photocatalytic degradation of SMT under visible light irradiation. Products, labeled P1-P9 were identified by UPLC-Q-TOF MS. ....	16

### FIGURES

Fig. S1. High-resolution XPS spectra of as-prepared samples: (a) C 1s, (b) O 1s. ....	19
Fig. S2. UPS spectra of PhC <sub>2</sub> Cu and AMO.....	20
Fig. S3. Tauc plots of PhC <sub>2</sub> Cu and AMO. ....	21
Fig. S4. Time-resolved fluorescence decay spectra. ....	22
Fig. S5. Adsorption experiments of different samples in the dark.....	23
Fig. S6. Comparison of H <sub>2</sub> O <sub>2</sub> generation by the PhC <sub>2</sub> Cu, AMO and PAM40 systems under the same conditions. ....	24
Fig. S7. (a) Cyclic voltammogram of PhC <sub>2</sub> Cu. (b). Mott–Schottky curves of AMO at 800 HZ. ....	25
Fig. S8. Schematic illustration of conventional type II heterojunctions. ....	26
Fig. S9. The UV absorption spectra of NBT after 30 min in photocatalytic process. ....	27
Fig. S10. TOC removal rate of SMT solution following 240 min of light exposure. ....	28
Fig. S11. Developmental toxicity of SMT and degradation intermediates/products. ....	29
<b>REFERENCES .....</b>	<b>30</b>

**Text S1. Chemical reagents**

Sulfamethazine (SMT), sulfisoxazole (SIZ), sulfathiazole (STZ), indomethacin (IDM), diclofenac (DCF), silver nitrate ( $\text{AgNO}_3$ ),  $\text{CuCl}_2 \cdot 2\text{H}_2\text{O}$ ,  $\text{Et}_3\text{N}$ , phenyl acetylene,  $\text{Ti}(\text{SO}_4)_2$  and  $\text{Na}_2\text{MoO}_4 \cdot 2\text{H}_2\text{O}$  were obtained from Aladdin Reagent Co. Ltd. (Shanghai, China). Isopropanol (IPA), 4-hydroxy-2,2,6,6-tetramethylpiperidinyloxy (TEMPO),  $\text{H}_2\text{O}_2$  and other analytical grade reagents were obtained from Taitan (China) and used without further purification. Sodium hydroxide (NaOH), hydrochloric acid (HCl) were purchased from Guangzhou Chemical Reagent Factory (Guangzhou, China). Methanol and acetonitrile of HPLC grade were purchased from CNW Technologies GmbH (Germany).

## **Text S2.** Characterization methods

The crystal phases of the photocatalysts were analyzed using a Bruker AXS D8 X-ray diffractometer with Cu K $\alpha$  radiation. Scanning electronic microscopy (SEM, Hitachi S4800) and transmission electron microscopy (TEM, JEM-2100HR) equipped with an energy dispersive spectrometer (EDS) were employed to study the morphologies of the as-prepared samples. X-ray photoelectron spectroscopy (XPS, Escalab 250Xi) equipped with Mg-K $\alpha$  radiation was used to examine the chemical states of the samples. The UV-vis absorption spectra were determined by a UV-vis-NIR spectrophotometer (UV-3600Plus, Shimadzu, Japan) using BaSO<sub>4</sub> as the reflectance standard. The photoluminescence (PL) spectra were monitored with a F97pro fluorescence spectrophotometer under 360 nm excitation. Transient photoluminescence decay spectra were recorded with an Edinburgh FS5 fluorescence lifetime spectrophotometer. The total organic carbon (TOC) was detected with a TOC analyzer (TOC-V CPH E200 V, Shimadzu, Japan).

The electrochemical and photoelectrochemical tests were performed on an electrochemical workstation (CHI-760E, China) with a conventional three-electrode system in 0.1 M Na<sub>2</sub>SO<sub>4</sub> electrolyte (pH = 5.9). A saturated calomel electrode (SCE), a platinum foil, and an ITO electrode deposited with samples were used as the reference electrode, counter electrode, and working electrode, respectively. The working electrode was prepared as follows: 10 mg of the sample was added in a mixture containing 50  $\mu$ L 10% Nafion and 1 mL ethanol, and then sonicated for 30 min to form a slurry. The slurry was coated onto the surface of the ITO glass and allowed to dry

naturally. For transient photocurrent response test, a 450 nm blue LED lamp was utilized as the light source. The electrochemical impedance spectra (EIS) were recorded in the frequency range of  $10^{-2}$  to  $10^5$  Hz, and Mott-Schottky plots were collected at different frequencies of 500 and 1000 Hz.

**Text S3.** Photocatalytic test and determination of SMT concentration

SMT was employed as a model antibiotic pollutant to assess the photocatalytic capacities of the as-prepared samples under blue LED exposure. Prior the light irradiation, a 20 mg sample of the photocatalysts was dispersed in 50 mL of a 10 mg/L SMT aqueous solution and magnetically stirred for 30 min in darkness to achieve adsorption-desorption equilibrium. During light exposure, 1 mL volumes of the reaction solution were extracted and filtered at predetermined intervals.

The PPCP concentrations were determined using Shimadzu LC 20A high performance liquid chromatography (HPLC, Japan), equipped with a C18 reversed-phase column (Zorbax Eclipse, 4.6 × 250 mm, 5 μm). The temperature of column was kept at 35°C and the injection volume was set at 20 μL. The detection wavelength of the UV detector was 262 nm. The isocratic mobile phase was made up of 70% methanol and 30% water (with 0.2% formic acid) at a flow rate of 1.0 mL min<sup>-1</sup>.

**Text S4.** Active species quantified and contributions rates of the ROS

The reactive oxygen species (ROS) generated during the photocatalytic processes were directly quantified using an ESR spectrometer (JES-FA200, Bruker Co., Germany), where 5,5-dimethyl-1-pyrroline N-oxide (DMPO) was used as the trapping reagent for superoxide radicals ( $O_2^{\bullet-}$ ) and hydroxyl radicals ( $\bullet OH$ ). To investigate the contribution rates of the reactive species to the degradation of SMT, a scavenger-quenching experiment was conducted using isopropyl alcohol (IPA), 2,2,6,6-Tetramethyl-1-piperidinyloxy (TEMPO) and methanol as scavengers for  $O_2^{\bullet-}$ ,  $\bullet OH$ , and  $h^+$ , respectively <sup>1</sup>. Further, the contributions of the RSs to the photocatalytic degradation of SMT were calculated using the equations below:

$$R_{O_2^{\bullet-}} = \frac{k_{O_2^{\bullet-}}}{k_{blank}} \approx \frac{k_{blank} - k_{TEMPO}}{k_{blank}} \quad (1)$$

$$R_{\bullet OH} = \frac{k_{\bullet OH}}{k_{blank}} \approx \frac{k_{blank} - k_{IPA}}{k_{blank}} \quad (2)$$

$$R_{h^+} = \frac{k_{h^+}}{k_{blank}} \approx \frac{k_{blank} - k_{Methanol}}{k_{blank}} \quad (3)$$

In Eqs. (1)-(3), R represents the fractional contribution of a particular reactive species to the apparent rate constant ( $k_{blank}$ ), and  $k_i$  is the rate constant of the degradation of SMT by a certain reactive species, or in the presence of a trapping reagent <sup>2</sup>.

**Text S5.** Detection of H<sub>2</sub>O<sub>2</sub>

The H<sub>2</sub>O<sub>2</sub> concentration was determined via a (p-hydroxyphenyl) acetic acid (PPOHPAA) technique. Typically, 2.7 mg POHPAA and 1.0mg horseradish peroxidase were mixed in a 10 mL aqueous solution that contained a potassium hydrogen phthalate buffer solution (8.2 g/ L), which was employed as fluorescent reagent. During the photocatalytic test in DI water, 2.0 mL of the reaction suspension were extracted and filtered at predetermined time intervals. Subsequently, 50 μL of the fluorescent reagent was added to the obtained solution and allowed to stand for 10min. The product of the reaction between H<sub>2</sub>O<sub>2</sub> and the fluorescent reagent (maximum emission at 409nm) could be detected by PL under 315 nm excitation<sup>3</sup>.

**Text S6.** The methods of theoretical calculations

SMT molecules were constructed in Gaussian 09 and optimized using the 6-31 G (d, p) basis set (B3LYP/6-311 G + (d, p)) in the hybrid density functional B3LYP method. The positions of HOMO (Highest occupied molecular orbital) and LUMO (Lowest unoccupied molecular orbital) of SMT molecule were determined <sup>4</sup>.

**Text S7.** Identification of photocatalytic degradation intermediates

The photocatalytic degradation intermediates of Sulfamethazine (SMT) were identified by ultraperformance liquid chromatography with quadrupole time-of-flight mass spectrometry (UHPLC-Q-TOF-MS, Thermo Scientific Ultimate 3000 RSLC and Q Exactive Orbitrap, USA). A Hypersil GOLD C18 column (100 x 2.1 mm, 1.9  $\mu\text{m}$ ) was used to separate the samples. The column temperature was maintained at 40°C and the injection volume was 5  $\mu\text{L}$ . The elution was performed using  $\text{H}_2\text{O}$  containing 0.1 % (v/v) formic acid as eluent A and methanol as eluent B at a flow rate of 0.3  $\text{mL min}^{-1}$ . Mass spectral analysis was conducted in both positive and negative mode, and the scan range of the mass spectrum was  $m/z$  50-750 <sup>5</sup>.

**Text S8.** The fitting method for time-resolved fluorescence decay spectroscopy

The fluorescence decay curves of the PhC<sub>2</sub>Cu and PAM40 were fitted using the triple-exponential function:

$$R(t) = B_1 \exp\left(-\frac{t}{\tau_1}\right) + B_2 \exp\left(-\frac{t}{\tau_2}\right) + B_3 \exp\left(-\frac{t}{\tau_3}\right)$$

where  $B_1$ ,  $B_2$ , and  $B_3$  are the pre-exponential factor, and  $\tau_1$ ,  $\tau_2$ , and  $\tau_3$  are the radiative lifetime.

The specific fitting data is given in Table S1. The average radiative lifetime ( $\tau_{ave}$ ) can be calculated by the following equation:

$$\tau_{ave} = \frac{B_1 \tau_1^2 + B_2 \tau_2^2 + B_3 \tau_3^2}{B_1 \tau_1 + B_2 \tau_2 + B_3 \tau_3}$$

**Table S1.** The fitted fluorescence decay components of PhC<sub>2</sub>Cu and PAM40.

Sample	$\tau_1$	$\tau_2$	$\tau_3$	B <sub>1</sub>	B <sub>2</sub>	B <sub>3</sub>	Average radiative lifetime (ns)
PhC <sub>2</sub> Cu	0.2779	1.5793	10.3560	0.036(20.63%)	0.006(20.91%)	0.003(58.46%)	9.82
PAM40	0.0481	1.4957	6.1645	0.265(37.54%)	0.006(26.81%)	0.002(35.65%)	1.22

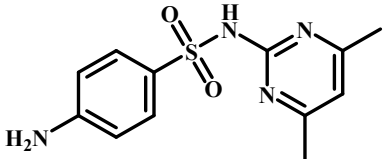
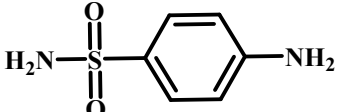
**Table S2. Comparison of reported literature on photocatalytic reduction of SMT**

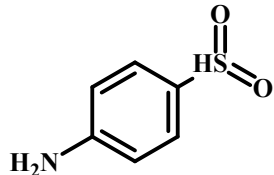
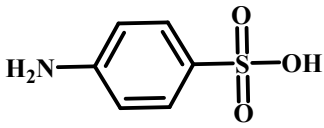
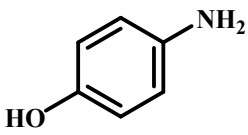
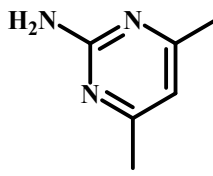
Photocatalyst	Dosage	Initial SMT concentration	Light source	$K_{\text{obs}}$ ( $\text{min}^{-1}$ )	Photocatalytic performance	CB (vs. NHE)	VB (vs. NHE)	Ref.
<b>PhC<sub>2</sub>Cu/Ag/Ag<sub>2</sub>MoO<sub>4</sub></b>	0.4 g/L	10 mg/L	9 W LED lamp (455 nm)	0.1622	97.70 % (20 min)	-2.20 eV	3.08 eV	Our work
<b>AgI/Bi<sub>4</sub>V<sub>2</sub>O<sub>11</sub></b>	1.0 g/L	10 mg/L	300 W Xenon lamp (>420 nm)	0.0431	91.47 % (60 min)	-0.40 eV	2.97 eV	6
<b>LCN</b>	0.5 g/L	100 $\mu$ M	300 W Xenon lamp (>420 nm)	0.1062	99.70% (60 min)	-1.04 eV	1.51 eV	7
<b>BCM/g-C<sub>3</sub>N<sub>4</sub></b>	1.0 g/L	10 mg/L	300 W Xenon lamp (>420 nm)	-	90.00 % (60 min)	-0.79 eV	1.23 eV	8
<b>O-C<sub>3</sub>N<sub>4</sub></b>	1.0 g/L	10 mg/L	200W LED lamp (420 nm)	-	96.54 % (120 min)	-0.72 eV	1.58 eV	9

<b>AgCl/MIL-100(Fe)</b>	0.5 g/L	1 mg/L	500 W Tungsten lamp (>400 nm)	0.03969	99.50 % (120 min)	-0.61eV	3.02eV	4
<b>F-TiO<sub>2</sub>/g-C<sub>3</sub>N<sub>4</sub></b>	0.5 g/L	10 mg/L	300 W Xenon lamp (>420 nm)	0.0435	>98 % (60 min)	-1.06eV	2.63eV	10
<b>Bi<sub>2</sub>O<sub>3</sub>-TiO<sub>2</sub></b>	1.0 g/L	20 mg/L	300 W Xenon	0.0291	100 % (120 min)	-	-	11
<b>CN-SA</b>	0.5 g/L	10 mg/L	300 W Xenon lamp (>420 nm)	0.0823	99 % (60 min)	-0.76eV	1.64 eV	12
<b>m-Bi<sub>2</sub>O<sub>4</sub>-P</b>	0.4 g/L	8 mg/L	350 W Xenon lamp (>420 nm)	0.0710	- (60 min)	-0.75eV	1.38 eV	13
<b>CuFe<sub>2</sub>O<sub>4</sub>/MXene (CFO/Ti<sub>3</sub>C<sub>2</sub>)</b>	0.5 g/L	40 mg/L	300 W Xenon lamp (>420nm)	0.0128	70 % (70 min)	-1.12eV	0.31eV	14

---

**Table S3.** Transformation products from the photocatalytic degradation of SMT under visible light irradiation. Products, labeled P1-P9 were identified by UPLC-Q-TOF MS.

Name	Retention time (min)	[M+H] <sup>+</sup>	Molecular weight (Da)	Chemical formula	Probable structure
SMT	7.07	279.0907	278	C <sub>12</sub> H <sub>14</sub> N <sub>4</sub> O <sub>2</sub> S	
P1	17.52	173.0783	172	C <sub>6</sub> H <sub>8</sub> N <sub>2</sub> O <sub>2</sub> S	

P2	11.82	158.1539	157	$C_6H_7NO_2S$	
P3	13.33	175.1481	174	$C_6H_7NO_3S$	
P4	13.33	111.0442	110	$C_6H_7NO$	
P5	6.89	124.0870	123	$C_6H_9N_3$	

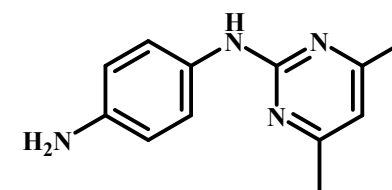
P6

4.28

215.1290

214

$C_{12}H_{14}N_4$



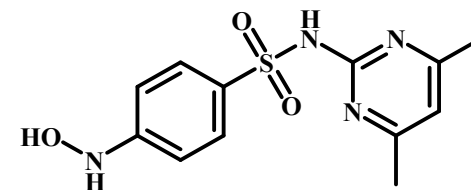
P7

14.13

295.2239

294

$C_{12}H_{14}N_4O_3S$



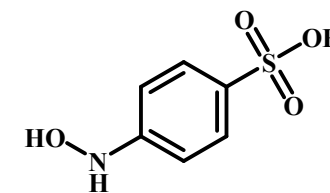
P8

2.03

190.9542

189

$C_6H_7NO_4S$



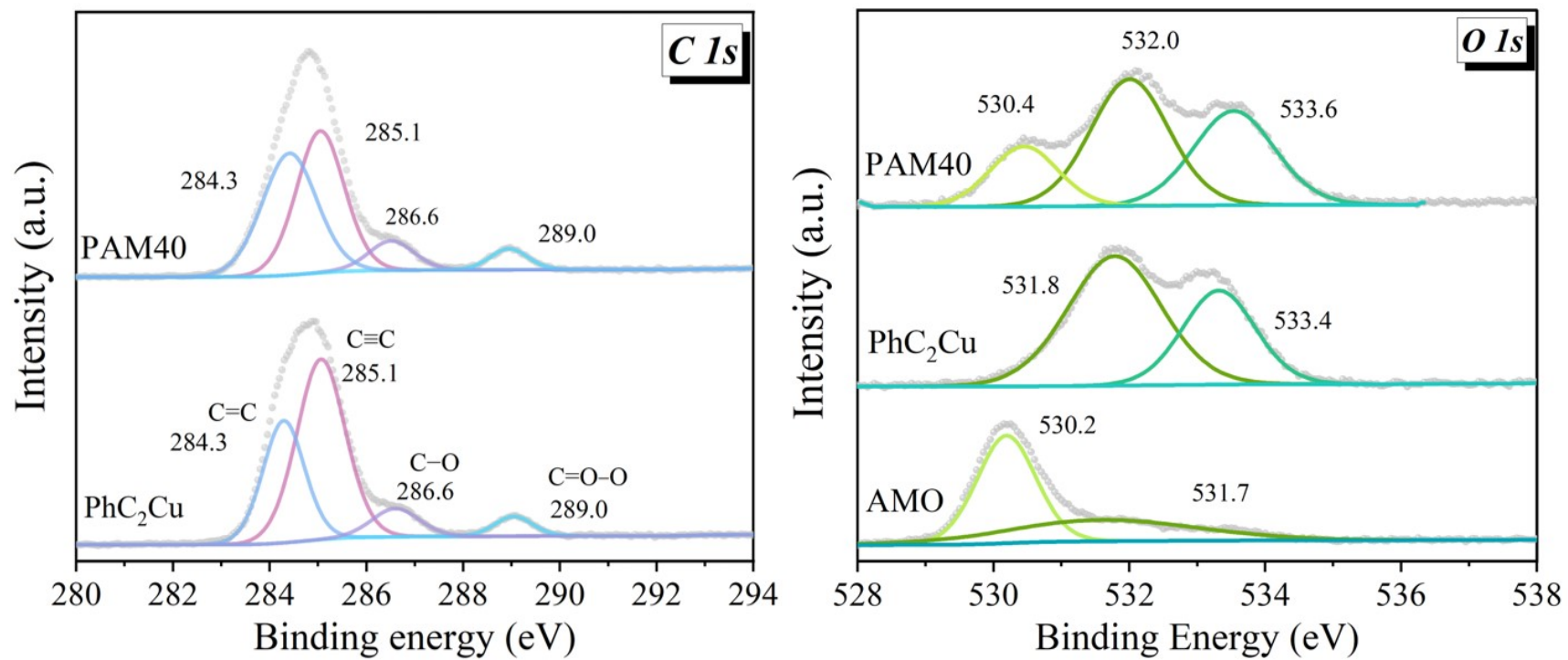


**Fig. S1.** High-resolution XPS spectra of as-prepared samples: (a) C 1s, (b) O 1s.

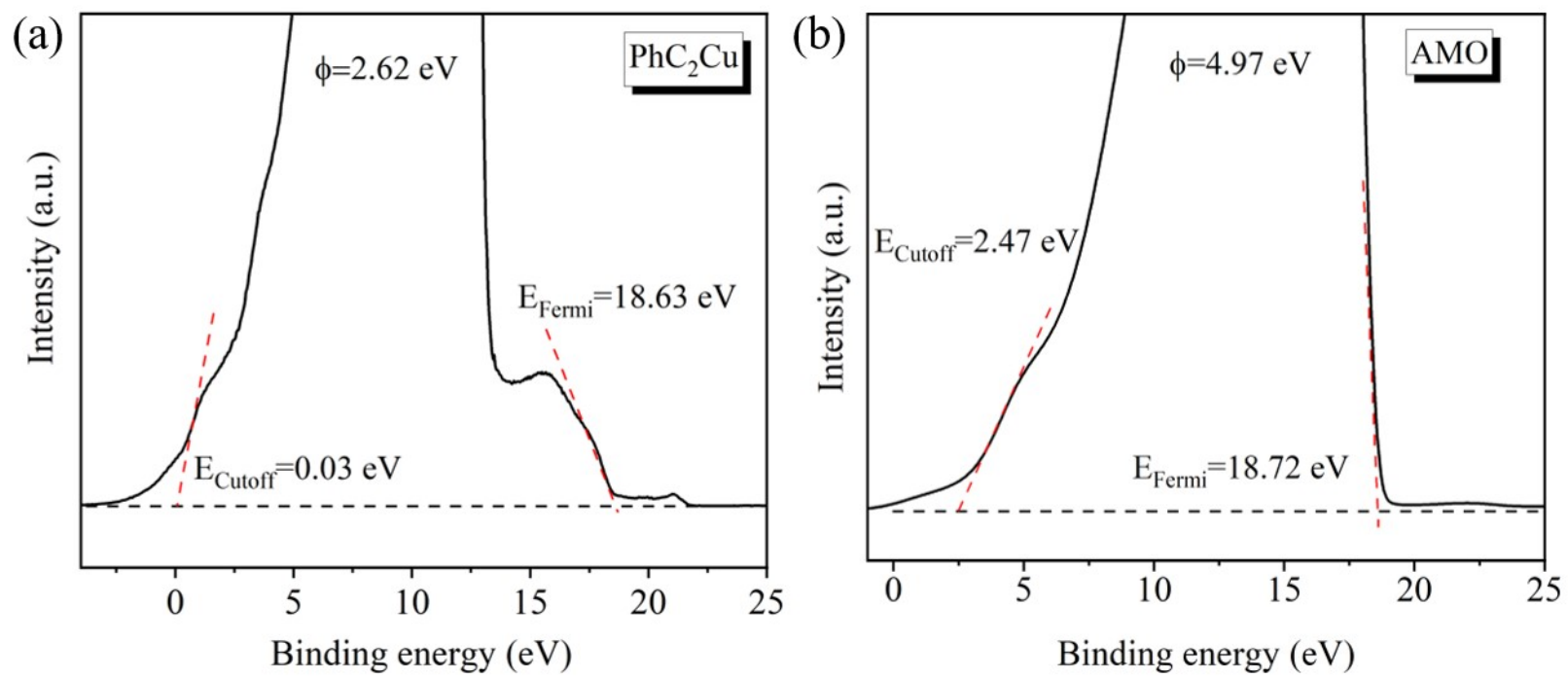


**Fig. S2.** UPS spectra of PhC<sub>2</sub>Cu and AMO.

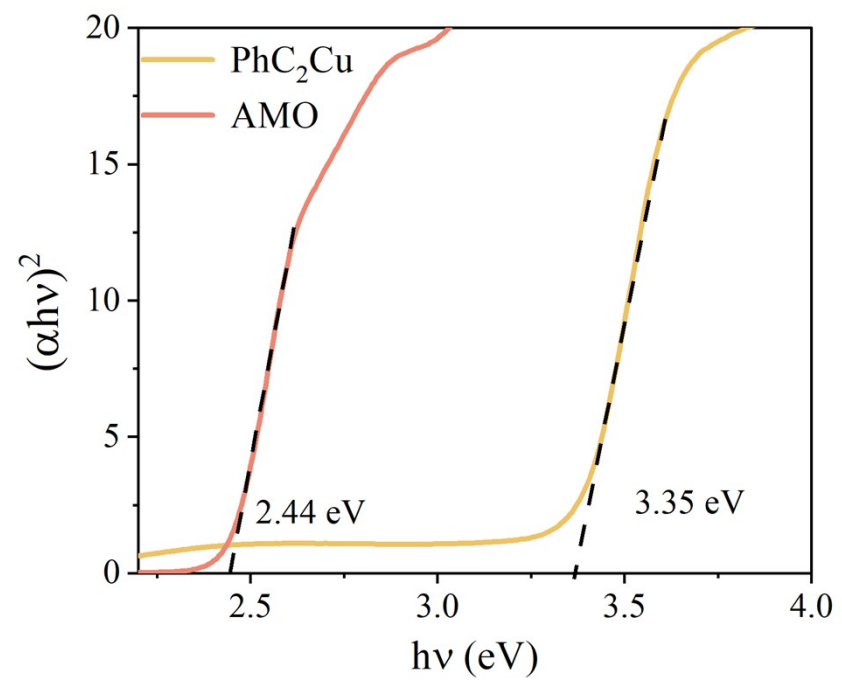


**Fig. S3.** Tauc plots of PhC<sub>2</sub>Cu and AMO.

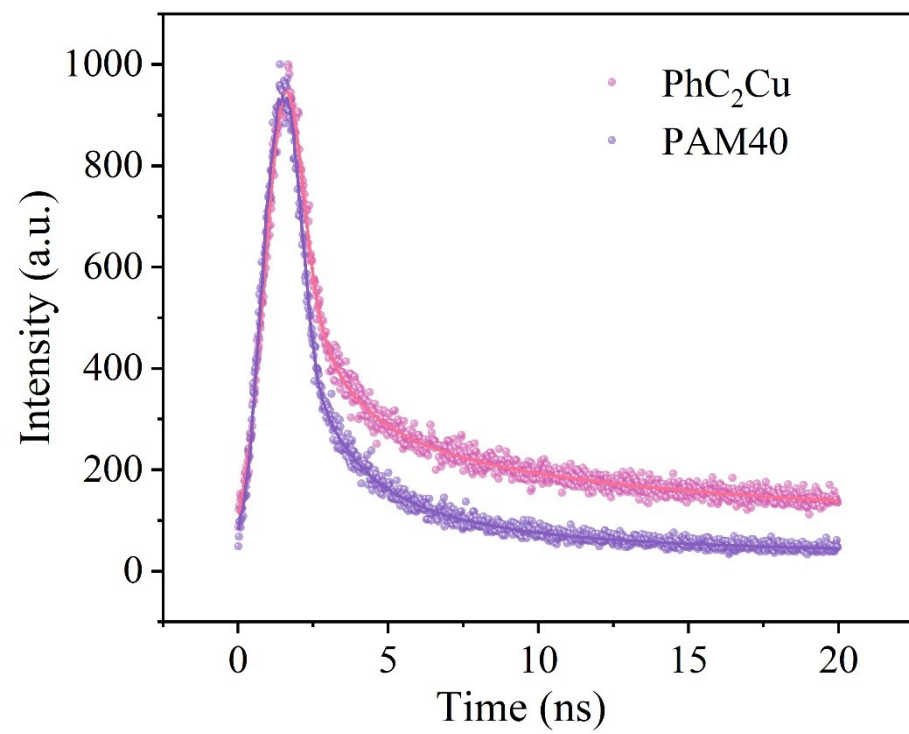


**Fig. S4.** Time-resolved fluorescence decay spectra.

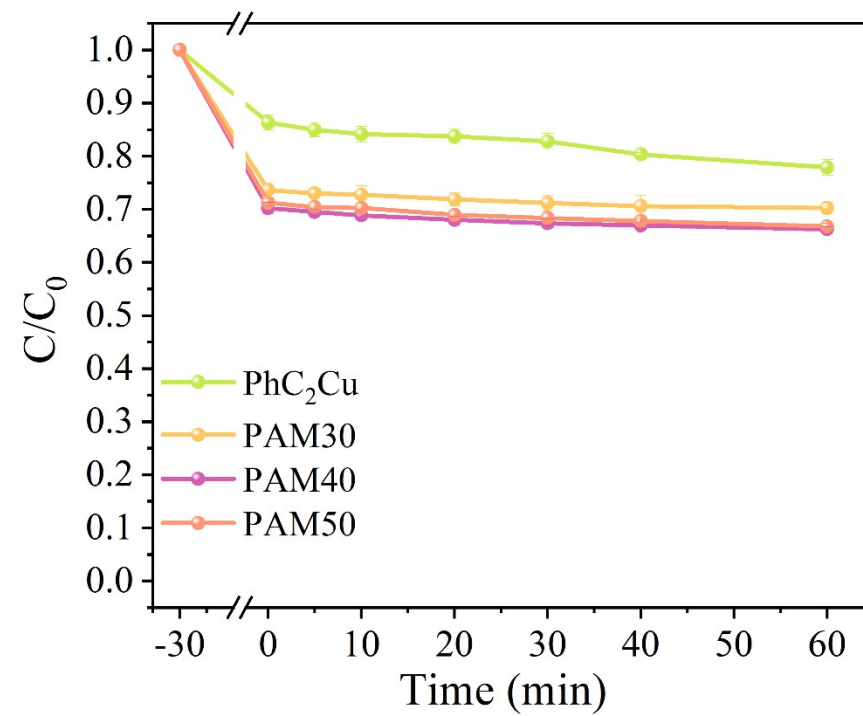


**Fig. S5.** Adsorption experiments of different samples in the dark.

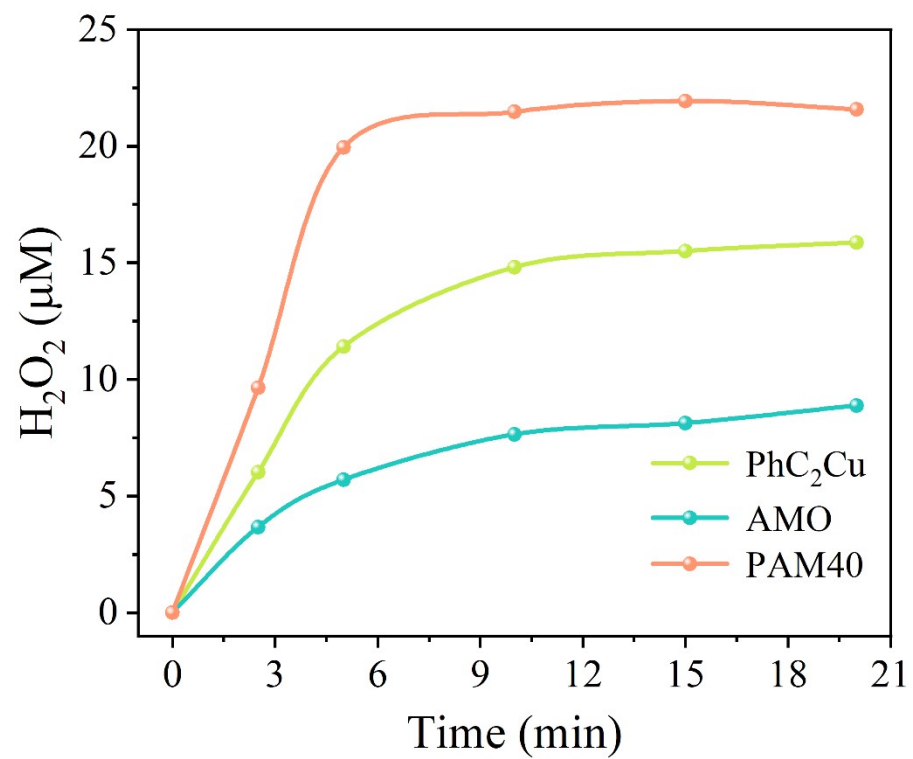


**Fig. S6.** Comparison of H<sub>2</sub>O<sub>2</sub> generation by the PhC<sub>2</sub>Cu, AMO and PAM40 systems under the same conditions.

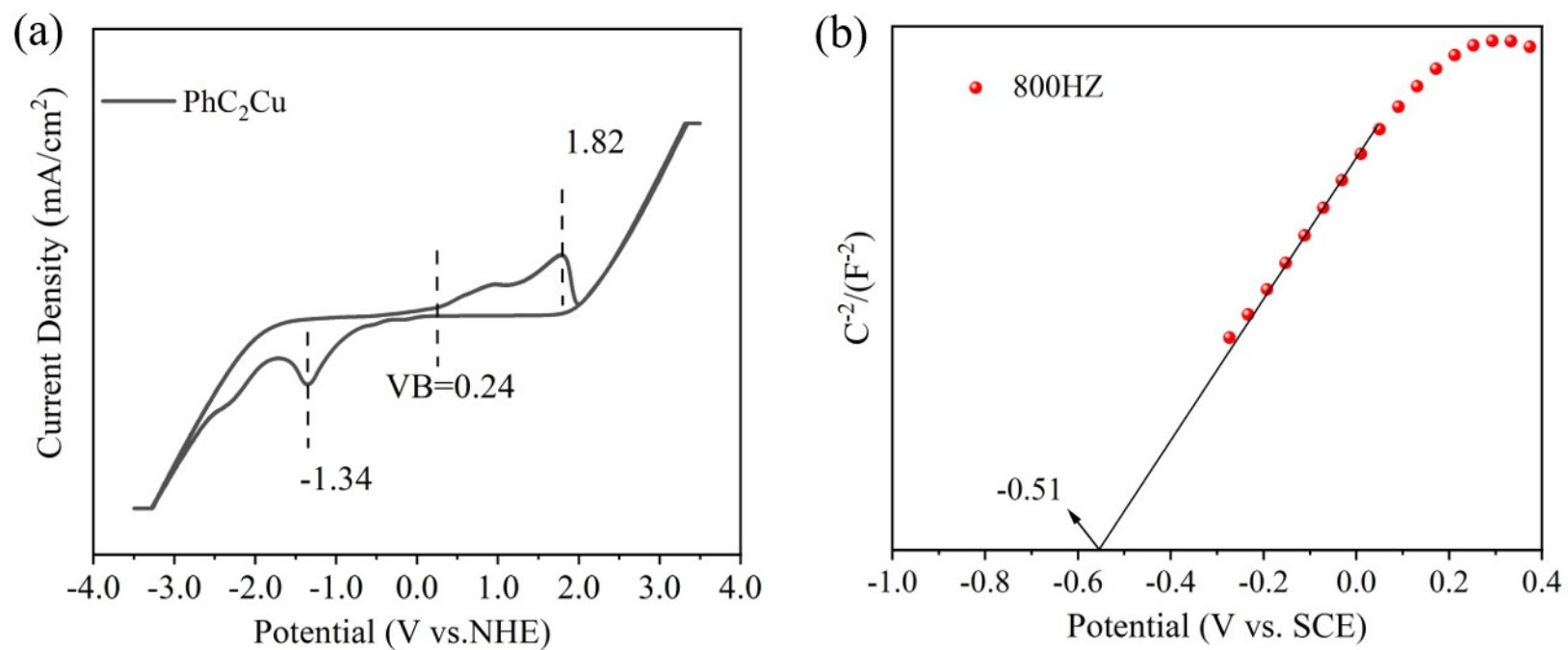


**Fig. S7.** (a) Cyclic voltammogram of PhC<sub>2</sub>Cu. (b). Mott-Schottky curves of AMO at 800 HZ.

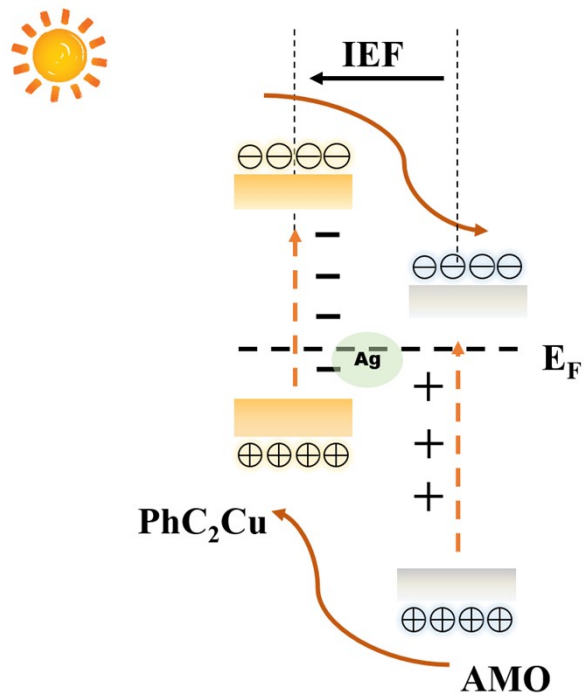


**Fig. S8.** Schematic illustration of conventional type II heterojunctions.

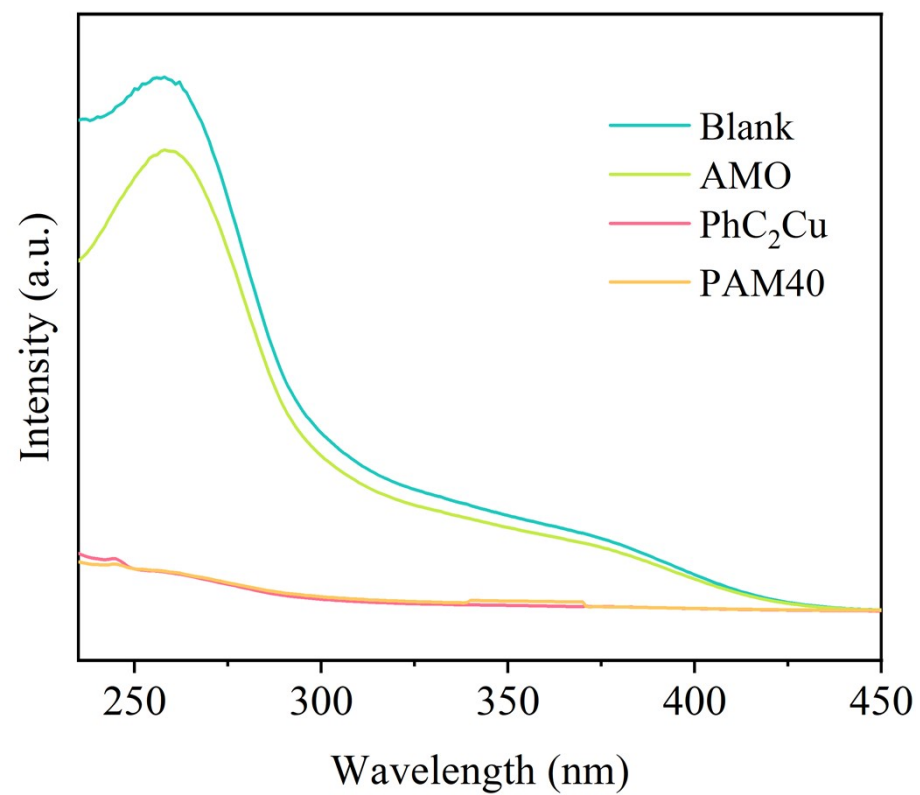


**Fig. S9.** The UV absorption spectra of NBT after 30 min in photocatalytic process.

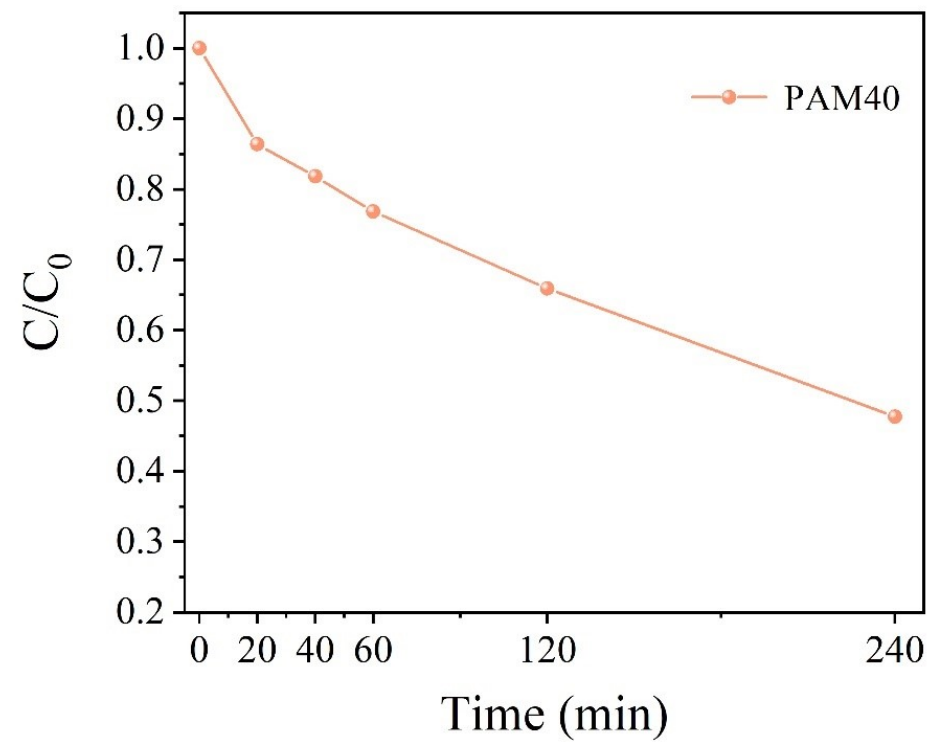


**Fig. S10.** TOC removal rate of SMT solution following 240 min of light exposure.

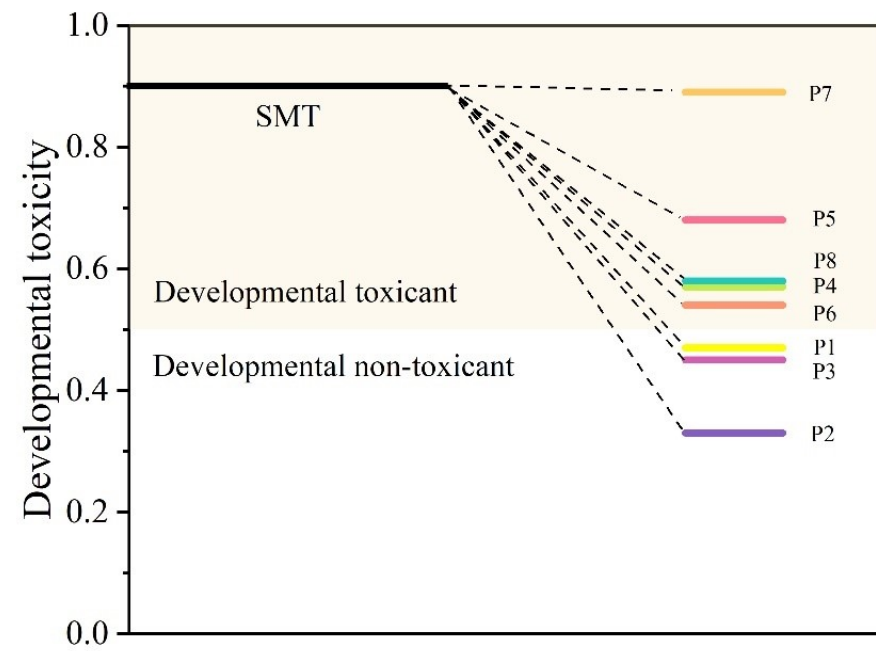


**Fig. S11.** Developmental toxicity of SMT and degradation intermediates/products.

## REFERENCES

1. D. Li, C. Wen, J. Huang, J. Zhong, P. Chen, H. Liu, Z. Wang, Y. Liu, W. Lv and G. Liu, High-efficiency ultrathin porous phosphorus-doped graphitic carbon nitride nanosheet photocatalyst for energy production and environmental remediation, *Applied Catalysis B: Environmental*, 2022, **307**.
2. J. Guo, H. Sun, X. Yuan, L. Jiang, Z. Wu, H. Yu, N. Tang, M. Yu, M. Yan and J. Liang, Photocatalytic degradation of persistent organic pollutants by Co-Cl bond reinforced CoAl-LDH/Bi(12)O(17)Cl(2) photocatalyst: mechanism and application prospect evaluation, *Water Res*, 2022, **219**, 118558.
3. X. Jin, Y. Wu, Z. Lin, D. Liang, F. Wang, X. Zheng, H. Liu, W. Lv and G. Liu, Plasmonic Ag nanoparticles decorated copper-phenylacetylide polymer for visible-light-driven photocatalytic reduction of Cr(VI) and degradation of PPCPs: Performance, kinetics, and mechanism, *J Hazard Mater*, 2022, **425**, 127599.
4. R. Ning, H. Pang, Z. Yan, Z. Lu, Q. Wang, Z. Wu, W. Dai, L. Liu, Z. Li, G. Fan and X. Fu, An innovative S-scheme AgCl/MIL-100(Fe) heterojunction for visible-light-driven degradation of sulfamethazine and mechanism insight, *J Hazard Mater*, 2022, **435**, 129061.
5. C. Tan, Q. Zhang, X. Zheng, H. Liu, P. Chen, W. Zhang, Y. Liu, W. Lv and G. Liu, Photocatalytic degradation of sulfonamides in 4-

phenoxyphenol-modified g-C<sub>3</sub>N<sub>4</sub> composites: Performance and mechanism, *Chemical Engineering Journal*, 2021, **421**.

6. X. J. Wen, L. Qian, X. X. Lv, J. Sun, J. Guo, Z. H. Fei and C. G. Niu, Photocatalytic degradation of sulfamethazine using a direct Z-Scheme AgI/Bi<sub>4</sub>V<sub>2</sub>O<sub>11</sub> photocatalyst: Mineralization activity, degradation pathways and promoted charge separation mechanism, *J Hazard Mater*, 2020, **385**, 121508.

7. C. Zhou, Z. Zeng, G. Zeng, D. Huang, R. Xiao, M. Cheng, C. Zhang, W. Xiong, C. Lai, Y. Yang, W. Wang, H. Yi and B. Li, Visible-light-driven photocatalytic degradation of sulfamethazine by surface engineering of carbon nitride : Properties, degradation pathway and mechanisms, *Journal of Hazardous Materials*, 2019, **380**.

8. C. Zhou, C. Lai, D. Huang, G. Zeng, C. Zhang, M. Cheng, L. Hu, J. Wan, W. Xiong, M. Wen, X. Wen and L. Qin, Highly porous carbon nitride by supramolecular preassembly of monomers for photocatalytic removal of sulfamethazine under visible light driven, *Applied Catalysis B: Environmental*, 2018, **220**, 202-210.

9. Q. Wang, M. Xiao, Z. Peng, C. Zhang, X. Du, Z. Wang and W. Wang, Visible LED photocatalysis combined with ultrafiltration driven by metal-free oxygen-doped graphitic carbon nitride for sulfamethazine degradation, *J Hazard Mater*, 2022, **439**, 129632.

10. P. Chen, S. Di, X. Qiu and S. Zhu, One-step synthesis of F-TiO<sub>2</sub>/g-C<sub>3</sub>N<sub>4</sub> heterojunction as highly efficient visible-light-active catalysts for

tetrabromobisphenol A and sulfamethazine degradation, *Applied Surface Science*, 2022, **587**.

11. N. Wang, X. Li, Y. Yang, Z. Zhou, Y. Shang, X. Zhuang and T. Zhang, Two-stage calcination composite of Bi<sub>2</sub>O<sub>3</sub>-TiO<sub>2</sub> supported on powdered activated carbon for enhanced degradation of sulfamethazine under solar irradiation, *Journal of Water Process Engineering*, 2020, **35**.

12. C. Zhou, D. Huang, P. Xu, G. Zeng, J. Huang, T. Shi, C. Lai, C. Zhang, M. Cheng, Y. Lu, A. Duan, W. Xiong and M. Zhou, Efficient visible light driven degradation of sulfamethazine and tetracycline by salicylic acid modified polymeric carbon nitride via charge transfer, *Chemical Engineering Journal*, 2019, **370**, 1077-1086.

13. P. Chen, Q. Zhang, X. Zheng, C. Tan, M. Zhuo, T. Chen, F. Wang, H. Liu, Y. Liu, Y. Feng, W. Lv and G. Liu, Phosphate-modified m-Bi<sub>2</sub>O<sub>4</sub> enhances the absorption and photocatalytic activities of sulfonamide: Mechanism, reactive species, and reactive sites, *J Hazard Mater*, 2020, **384**, 121443.

14. Y. Cao, Y. Fang, X. Lei, B. Tan, X. Hu, B. Liu and Q. Chen, Fabrication of novel CuFe<sub>2</sub>O<sub>4</sub>/MXene hierarchical heterostructures for enhanced photocatalytic degradation of sulfonamides under visible light, *J Hazard Mater*, 2020, **387**, 122021.

15. Y.-C. Zhou, X.-Y. Xu, P. Wang, H. Fu, C. Zhao and C.-C. Wang, Facile fabrication and enhanced photocatalytic performance of visible light responsive UiO-66-NH<sub>2</sub>/Ag<sub>2</sub>CO<sub>3</sub> composite, *Chinese Journal of Catalysis*, 2019, **40**, 1912-1923.

16. W. Zhang, L. Wang and J. Zhang, Preparation of Ag UiO-66-NH<sub>2</sub> and its application in photocatalytic reduction of Cr(VI) under visible light, *Research on Chemical Intermediates*, 2019, **45**, 4801-4811.
17. Y.-X. Li, X. Wang, C.-C. Wang, H. Fu, Y. Liu, P. Wang and C. Zhao, S-TiO<sub>2</sub>/UiO-66-NH<sub>2</sub> composite for boosted photocatalytic Cr(VI) reduction and bisphenol A degradation under LED visible light, *Journal of Hazardous Materials*, 2020, **399**, 123085.
18. X. Wei, C. C. Wang, Y. Li, P. Wang and Q. Wei, The Z-scheme NH<sub>2</sub>-UiO-66/PTCDA composite for enhanced photocatalytic Cr(VI) reduction under low-power LED visible light, *Chemosphere*, 2021, **280**, 130734.